

Ectopic transient overexpression of *OCT-4* facilitates BMP4-induced osteogenic transdifferentiation of human umbilical vein endothelial cells

Seung Hyun L Kim¹, Seunghun S Lee¹ , Inseon Kim², Janet Kwon¹, Song Kwon², Taegeun Bae³, Junho Hur⁴, Hwajin Lee⁵ and Nathaniel S Hwang^{1,2,3} 

Abstract

Limitation in cell sources for autologous cell therapy has been a recent focus in stem cell therapy and tissue engineering. Among various research advances, direct conversion, or transdifferentiation, is a notable and feasible strategy for the generation and acquirement of wanted cell source. So far, utilizing cell transdifferentiation technology in tissue engineering was mainly restricted at achieving single wanted cell type from diverse cell types with high efficiency. However, regeneration of a complete tissue always requires multiple cell types which poses an intrinsic complexity. In this study, enhanced osteogenic differentiation was achieved by transient ectopic expression of octamer-binding transcription factor 4 (*OCT-4*) gene followed by bone morphogenetic protein 4 treatment on human umbilical vein endothelial cells. *OCT-4* transfection and bone morphogenetic protein 4 treatment resulted in enhanced expression of osteogenic markers such as core-binding factor alpha 1, alkaline phosphatase, and collagen I compared with bone morphogenetic protein 4 treatment alone. Furthermore, we employed gelatin-heparin cryogel in cranial defect model for in vivo bone formation. Micro-computed tomography and histological analysis of in vivo samples showed that *OCT-4* transfection followed by bone morphogenetic protein 4 treatment resulted in efficient transdifferentiation of endothelial cells to osteogenic cells. These results suggest that the combination of *OCT-4* and bone morphogenetic protein 4 on endothelial cells would be a reliable multicellular transdifferentiation model which could be applied for bone tissue engineering.

Keywords

Transdifferentiation, bone regeneration, osteogenesis, bone tissue engineering, cell therapy

Received: 30 September 2019; accepted: 7 February 2020

Introduction

Bone is a highly vascularized heterogeneous tissue consisting of both osteogenic and angiogenic cells. Thus, multiple cell types are needed to achieve complete bone tissue

engineering. Recent studies have discovered importance of angiogenesis in bone regeneration.^{1–5} Vascularization provides oxygen and nutrients, which are essential for cell growth, and studies have shown correlation between low osteogenic efficiency and low in vivo vascularization.⁶

¹Interdisciplinary Program in Bioengineering, Seoul National University, Seoul, Republic of Korea

²School of Chemical and Biological Engineering, Institute of Chemical Processes, Seoul National University, Seoul, Republic of Korea

³BioMAX/N-Bio Institute, Seoul National University, Seoul, Republic of Korea

⁴Department of Medicine, Kyung Hee University, Seoul, Republic of Korea

⁵School of Dentistry, Seoul National University, Seoul, Republic of Korea

Corresponding authors:

Hwajin Lee, School of Dentistry, Seoul National University, Seoul 08826, Republic of Korea.
Email: hwajin2k@gmail.com

Nathaniel S Hwang, Interdisciplinary Program in Bioengineering, Seoul National University, Seoul 08826, Republic of Korea.
Email: nshwang@snu.ac.kr



However, difficulty in controlling directed differentiation of multiple cell types is a limitation in tissue engineering. Here, we aimed to provide a protocol that can generate complete bone tissues composed of multiple cell types from a single cell source.

Somatic cell reprogramming has shown plasticity in adult somatic cells as well as demonstrating the possibility of generating various cell types in unlimited numbers.^{7,8} To induce somatic cell plasticity, sets of transcription factors were proposed, including Yamanaka factors, which consist of *OCT3/4*, *SOX2*, *C-MYC*, and *KLF4*, and Thomson factors which are *OCT-4*, *SOX2*, *NANOG*, and *LIN28*.^{9,10} In particular, *OCT-4* is considered as an essential factor in reprogramming cells. A study by Szabo et al.¹¹ demonstrated ectopic expression of *OCT-4* in human dermal fibroblasts induced transdifferentiation into multilineage blood progenitors. A recent work by Yamamoto et al.¹² discovered *OCT-4* alone significantly increased alkaline phosphatase (*ALP*) and osteocalcin (*OCN*) RNA expressions as well as strong von Kossa's staining. The article further highlights significance of *OCT-4* in transdifferentiating human fibroblasts into osteoblast-like cells.

Transforming growth factor family, especially bone morphogenetic protein type 4 (*BMP4*), is often used in inducing osteogenesis in cells.^{13–15} Another important factor is SMAD activation which is a key contributor for bone homeostasis. Recently, *BMP4* phosphorylation of activin-like kinase 2 (*ALK2*) resulting in SMAD activation was achieved and caused endothelial-mesenchymal transition (*EndMT*). In 2010, Medici et al.¹⁶ examined *EndMT* in a pathological condition called fibrodysplasia ossificans progressiva (*FOP*) in which heterotopic ossification occurs in soft tissues. Molecular mechanism investigation discovered *TGF- β 2* and *BMP4* treatment for 48 h induce *ALK2* receptor phosphorylation which caused the same kind of *EndMT* occurred in *FOP*. Phosphorylation of *ALK2* results in R-SMAD, SMAD1/5/8, activation which forms a complex with CO-SMAD, SMAD4. Together, this complex promotes osteogenic gene transcription.

For in vivo bone tissue regeneration, cryogels were used for simple delivery purposes. Cryogels allow macroporous formation that provides favorable cell niche in which seeded cells have enough space to proliferate and host cells can migrate into.^{17,18} Previously, our laboratory has developed macroporous gelatin-heparin (*GH*) cryogel.¹⁹ Our cells treated with *OCT-4* followed by *BMP4* were seeded onto *GH* scaffold for in vivo bone formation. Taken together, we report the effective transdifferentiation using *OCT-4* and *BMP4* treatments on human umbilical vein endothelial cells (*HUVECs*) and formation of a complex bone tissue in vivo from single cell source.

Materials and methods

Cell culture

HUVECs (Lonza, C2519A) were grown in EGM-2 medium (Lonza) on 0.1% gelatin (Sigma-Aldrich) plates. For serum-free media, all growth factor supplements and FBS in EGM-2 kit (Lonza) were not added. For osteogenesis, StemPro™ Osteogenesis medium (Thermo Fisher Scientific) was changed every 2–3 days.

Plasmid transfection

After reaching confluency, *HUVECs* were harvested for electroporation with Neon Transfection System (Thermo Fisher Scientific) with each electroporation sample containing 15 μ g of *OCT-4* plasmid DNA (Addgene #13366), 2×10^6 cells, and 100 μ L of resuspension buffer solution provided and recommended by the manufacturer. After plasmid gene delivery, cells were maintained at 37°C with 5% CO₂ for 2 days.

Growth factor treatment

Two days after transfection, cells were re-plated in 24 or 48 wells (SPL Life Sciences). One day after re-plating in the presence of fetal bovine serum (FBS), serum-free condition was maintained for 24 h. After 24-h culture in endothelial serum-free media (Lonza), recombinant *BMP4* growth factor (R&D Systems) was added in concentration of 10 ng/mL. *BMP4* was added for 48 h before switching into osteogenesis media.

RNA extraction, cDNA generation, and quantitative RT-PCR

Cells were collected and treated with Trizol® reagent (Thermo Fisher Scientific). After 20 min in ice, chloroform was added and samples were shaken for 15 s. Following 10 min of incubation in room temperature, samples were centrifuged at 15,000 r/min for 20 min at 4°C. Once solution separates into two layers, clear aqueous phase was collected and isopropanol was added for RNA precipitation. After 5 min of incubation in room temperature, precipitated RNA samples were collected through centrifugation at 15,000 r/min for 20 min at 4°C. For washing step, 75% ethanol was added to precipitated RNA pellet and centrifugation at 10,000 r/min for 10 min at 4°C. Washed RNA was denatured in molecular grade water (Sigma-Aldrich) at 60°C for 10 min. cDNA was generated through reverse-transcriptional PCR from collected RNA with cDNA kit (EZ006M, Enzynomics) as per the manufacturer's protocol. Concentration of cDNA was measured with Infinite® 200 PRO (Tecan). Quantitative RT-PCR was performed using SYBR green PCR Mastermix via StepOnePlus™

Real-Time PCR System (Applied Biosystems). All primers (CosmoGenetech) used for qRT-PCR is listed in Supplementary Table 3. The same protocol was used for RNA-Seq analysis.

Immunostaining

Cells were fixated with 4% paraformaldehyde (PFA; Sigma-Aldrich) for 20 min at room temperature. After washing twice with phosphate-buffered saline (PBS) for 5 min, samples were permeabilized with 0.2% Triton-X100 (Sigma-Aldrich) in 1% bovine serum albumin (BSA) (MP Biomedicals)/PBS for 15 min. Following permeabilization, blocking solution, 10% normal goat serum (NGS) (Vector Laboratories) in 1% BSA/PBS was added and incubated in room temperature for 1 h. For primary antibody treatment, samples were treated with OCT-4 (Abcam, ab19857) or OCN antibody (Abcam, ab13420) in 0.1% Triton-X100, 5% NGS, and 1% BSA/PBS solution overnight. After thorough washing, secondary antibody against mouse (1:200, Jackson Immuno Research) was treated for 1.5 h in the same solution components as primary antibody solution. DAPI staining was performed for nucleus detection by incubating samples in DAPI (1:200; D9541, Sigma-Aldrich) in PBS for 15 min. For histological immunostaining, the same protocol was followed except antigen retrieval solution, proteinase K (1:100; Sigma-Aldrich), was treated for 10 min in 37°C before permeabilization. Samples were imaged with confocal laser scanning microscopy (Zeiss) or EVOS (Thermo Fisher Scientific) and analyzed with ImageJ software (NIH). Originally merged confocal images were split into red fluorescent protein (RFP), green fluorescent protein (GFP), and DAPI channels for Figure 2(a) and (b) via ImageJ. Also, positively stained area was marked, and intensity was measured for mean fluorescence intensity quantification.

Alizarin Red S staining

Cells were fixated with 4% paraformaldehyde for 20 min at room temperature. After washing twice with distilled water for 5 min, Alizarin Red S (ARS) (ScienCell Research Laboratories) solution was treated for 30 min at room temperature. Samples were imaged with microscope (Olympus).

GH cryogel fabrication

GH cryogel was previously fabricated and used in a different study.¹⁹ 1-ethyl-3-(3-(dimethylamino)propyl)carbodiimide (EDC) (Thermo Fisher Scientific) and sulfohydroxysuccinimide (NHS) (Thermo Fisher Scientific) were dissolved in deionized (DI) water at 50 and 25 mM concentration, respectively. EDC and NHS were used as

cross-linking reagents for gelatin/heparin solution which was type A gelatin (from porcine skin, Sigma-Aldrich) and heparin (Merck Millipore) in DI water with final concentration of 1% (w/v) gelatin and 0.3% (w/v) heparin. After mixing these solutions, 200 μ L was aliquoted into pre-chilled mold and stored in -20°C overnight for ice crystals to form. Then, samples were lyophilized for macroporous structure formation and stored away until use. Before seeding cells, GH cryogels were punched in 3.5-mm diameter size with 3.5-mm biopsy punch (Miltex) so that the size of cryogels would fit in cranial defect area.

Cell viability and proliferation on gel

One day after seeding 0.1 or 0.2 million cells on 3.5-mm diameter scaffold, cell viability was measured after one day with LIVE/DEAD[®] cell viability kit (Thermo Fisher Scientific). Dead cells were stained with ethidium homodimer-1, and live cells were stained with calcein AM after incubation for 30 min in 37°C with 5% CO₂. Images were captured with confocal laser scanning microscopy. Proliferation of cells was measured via Alamar blue assay (Thermo Fisher Scientific) following the manufacturer's protocol for days 1, 3, 5, and 7 after seeding on scaffold.

Histological assessment

Histological assessment was made via hematoxylin and eosin (H&E) and Masson's trichrome staining on paraffin-embedded samples. Before staining, mouse crania were fixed in 4% PFA for 24 h, decalcified with 0.5M EDTA, embedded in paraffin, and sectioned in 4 μ m thickness. These sectioned tissues were deparaffinated with xylene and gradually hydrated with different percentages of ethanol before any chemical or immunostaining.

Surgical protocol

All experiments followed the Guide for the Care and Use of Laboratory Animals by the Seoul National University. Mice were under Zoletil 50 (Virbac) and Rompun[®] injectable (Bayer) anesthesia, and minimal amount of animal suffering was made. Nude mice were used for all animal model experiments and were cared regularly in climate-controlled rooms at 22°C with 50% humidity and 12-h light/dark cycles. Cranial defect was made on 8-week-old nude mice in the center of sagittal crest with a 4-mm diameter dental drill after making a longitudinal incision with a surgical knife. Following the removal of dissected cranial piece, cell-seeded scaffold or acellular scaffold covered the defect area and skin was sutured with 6-0 Vicryl. Animals were carefully handled and were ultimately sacrificed with CO₂ gas 8 weeks after surgery.

Micro-computed tomography

Quantification of bone formation after surgery was measured with SkyScan 1172 (SkyScan) at 59 kV, 167 μ A, and 40 ms of exposure. Images were gathered every 0.6° with full rotation of 360°. All images were reconstructed and analyzed via ReCon Micro-CT software.

Statistical analysis

All data present mean \pm standard deviation (SD). Statistical significant differences were analyzed by one-way analysis of variance (ANOVA) followed by Tukey's post hoc test. *p* values less than 0.05 were recognized as statistically significant: **p* < 0.05, ***p* < 0.01, ****p* < 0.005.

Ethical statement

All experiments were performed in accordance with the Guide for the Care and Use of Laboratory Animals by the Seoul National University (SNU-170728-1-5). All participants were aware and in consent with guidelines provided from the aforementioned committee.

Results

Initial cellular response of transdifferentiation factors

Development of vascularized bone tissue normally requires two different lineages of cells, endothelial and mesenchymal, for angiogenesis and osteogenesis, respectively.²⁰ In this study, we developed a protocol that enables generation of bone cell types from a single cell source. Previous studies have shown ectopic *OCT-4* expression alone can induce conversion in cells and BMP4 can activate ALK2 by phosphorylation causing EndMT in endothelial cells.^{11,16} Based on these findings, we aimed to enhance the mesenchymal conversion through combining the primary transfection with transient ectopic *OCT-4* expression and subsequent BMP4 treatment. After *OCT-4* transfection and subsequent BMP4 treatment, cells underwent in vitro cell culture in osteogenic medium for 1 or 2 weeks or in vivo assessment in cranial defect model for 8 weeks. After electroporation of HUVECs, gene delivery was confirmed through traditional RT-PCR on exogenous *OCT-4* gene and immunocytochemistry showing ~93% of transfection rate (Figure 1(a)). The PCR band clearly shows the presence of exogenous *OCT-4* gene expression for transfected HUVECs compared with that of non-transfected cells. Immunocytochemistry also shows positive *OCT-4* protein expression. To induce further conversion, recombinant BMP4 was treated for 48 h on *OCT-4*-transfected cells. Duration of BMP4 treatment was determined based on a previous study by Medici et al. and was confirmed with cell morphology change and expressions of alpha-smooth muscle

actin staining in BMP4-treated samples (Figure 1(e) and (f)). For comparison, we examined the HUVECs that were only transfected with *OCT-4* plasmids without BMP treatment. In addition, we also examined the negative control HUVECs and HUVECs with BMP4 treatment only. Activation of BMP receptors from BMP4 treatment was observed with quantitative real-time PCR (Figure 1(b)). HUVECs transfected with *OCT-4* followed by BMP4 treatment showed somewhat increased gene expression of BMP-receptor IA (*BMPRIA*) and BMP-receptor II (*BMPRII*) (1.6-fold and 1.55-fold, respectively). After sequential *OCT-4* transfection and BMP4 treatment, cells' state become heterogeneous expressing both elevated EndMT and endothelial markers. Endothelial-mesenchymal transition markers such as snail family zinc finger 2 (*SLUG*) (2.5 fold) and snail family zinc finger 1 (*SNAIL*) (6 fold) in samples transfected with *OCT-4* followed by BMP4 treatment (Figure 1(c)). Interestingly, for the same group, expressions for endothelial markers did not decrease (Figure 1(d)). Instead, all three endothelial genes, *CD31*, vascular cell adhesion molecule 1 (*VCAMI*), and vascular endothelial growth factor receptor 2 (*VEGFR-2*), had elevated expressions by 3-, 1.5-, and 6-fold, respectively, for cells transfected with *OCT-4* and treated with BMP4 protein. Figure 1(f) shows immunocytochemistry staining for endothelial (CD31) and fibroblastic-mesenchymal (α -SMA) markers for all samples. Cells transfected with *OCT-4* followed by BMP4 treatment show high expressions for both endothelial and mesenchymal markers demonstrating those cells have dual characteristics. Thus, initial response of cells transfected with *OCT-4* followed by BMP4 treatment are at heterogeneous state with both mesenchymal and endothelial characteristics.

In vitro osteogenic transdifferentiation of HUVECs

After *OCT-4* transfection followed by BMP4 treatment, cells were cultured in osteogenic differentiation media for 7 or 14 days. One week of osteogenic media culture significantly upregulated expression of three main osteoblast-related genes, core-binding factor alpha 1 (*CBFA1*), *ALP*, and collagen 1 (*COL1*) (Figure 2(a); top). For *CBFA1*, expression elevated by sevenfold and sixfold for cells transfected with *OCT-4* followed by BMP4 treatment and cells with *OCT-4*-only, respectively. *COL1* expression also rose up to 14 fold for cells transfected with *OCT-4* followed by BMP4 treatment. Similarly, OCN protein expression from immunocytochemistry showed strongest for cells transfected with *OCT-4* followed by BMP4 treatment (Figure 2(a); bottom), demonstrating a successful transdifferentiation into osteogenic cell type. Quantification of immunofluorescence is shown as well. Similar to the gene expression data, cells with *OCT-4* only showed second strongest immunocytochemistry staining. This suggests

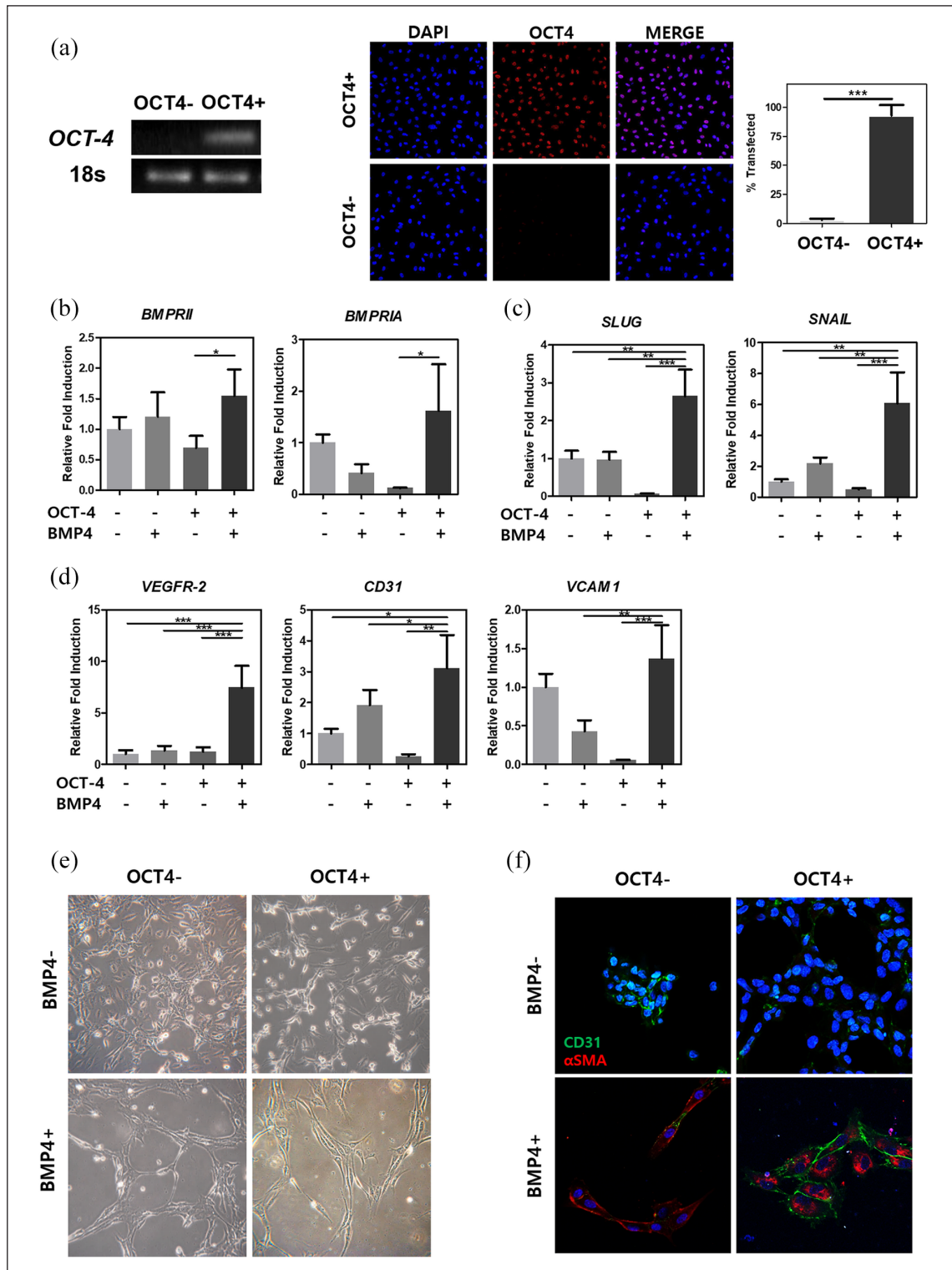


Figure 1. Confirmation after OCT-4 transfection and BMP4 growth factor treatment. (a) Gene expression and protein expression were examined after OCT-4 transfection in HUVECs. mRNA expression levels of BMP pathway receptors (b), endothelial-mesenchymal transition markers (c), and endothelial cell markers (d) were measured after sequential treatments. (e) Bright-field images showing different morphological change depending on transfection of OCT-4 and/or treatment of BMP4. (f) Immunocytochemical staining of cells showing endothelial marker, CD31, in green and/or mesenchymal marker, α -SMA, in red. HUVECs treated or not treated with either OCT-4 or BMP4 are represented with - or + sign. The full-length agarose gels are shown in Figure S1 in Supplementary Data.

Error bars show standard deviation on the mean for $n=3$: * $p < 0.05$; ** $p < 0.01$; *** $p < 0.001$. Scale bar = 25 μ m.

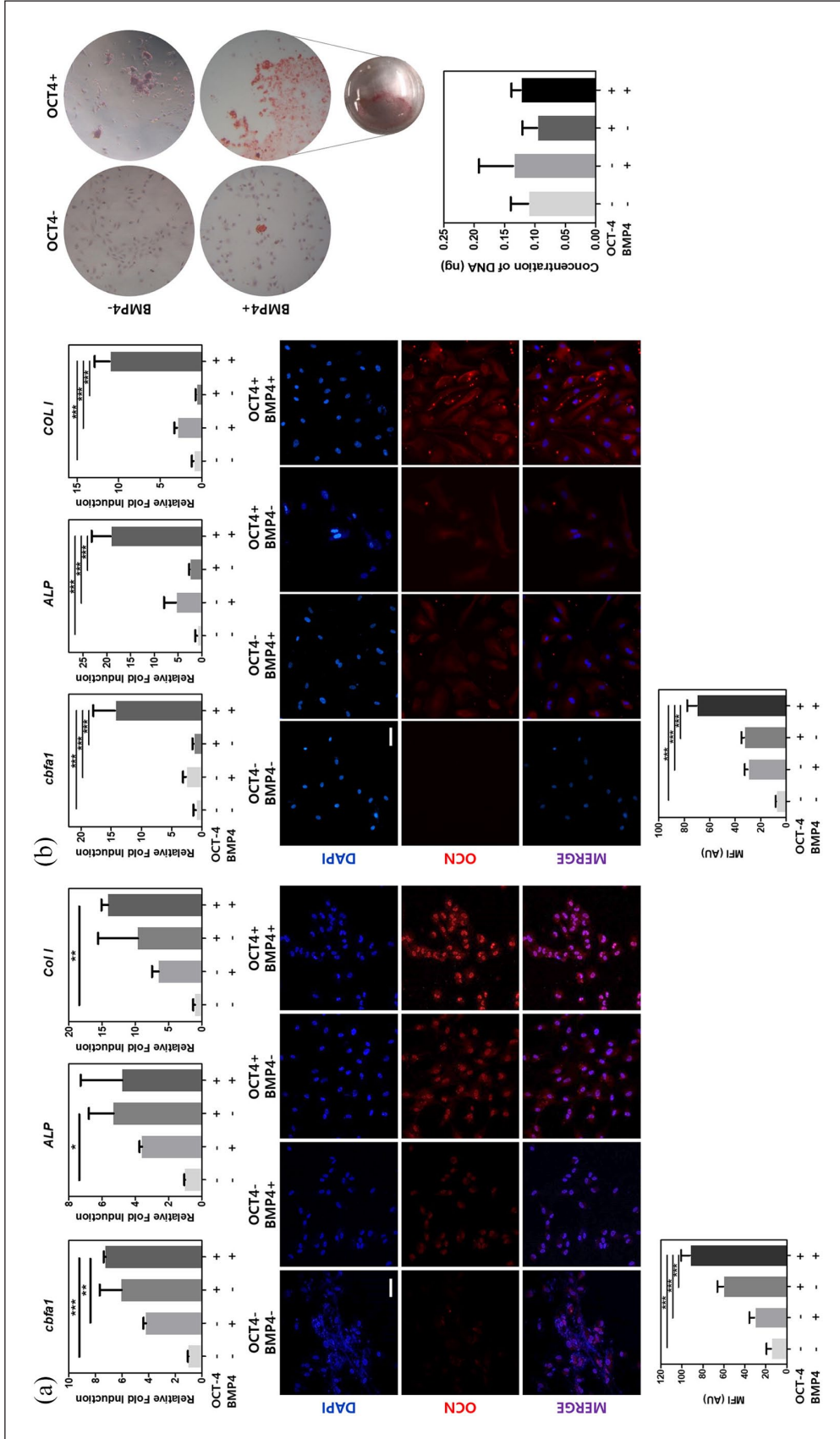


Figure 2. Sequential treatment of OCT-4 and BMP4 enhances in vitro osteogenic differentiation. (a) mRNA expression levels of osteogenic markers, *CBFA1*, *ALP*, and *COL1* were measured by real-time PCR and osteocalcin protein expression levels were shown through immunocytochemistry after 1 week of osteogenic differentiation. (b) mRNA expression levels of osteogenic markers, *CBFA1*, *ALP*, and *COL1* were measured by real-time PCR, osteocalcin protein expression levels were shown through immunocytochemistry, and calcification of cells were represented with ARS staining after 2 weeks of osteogenic differentiation. HUVECs treated or not treated with either OCT-4 or BMP4 are represented with - or + sign. Error bars show standard deviation on the mean for n=3: *p < 0.05; **p < 0.01; ***p < 0.001; ****p < 0.0001. Scale bar = 100 μm.

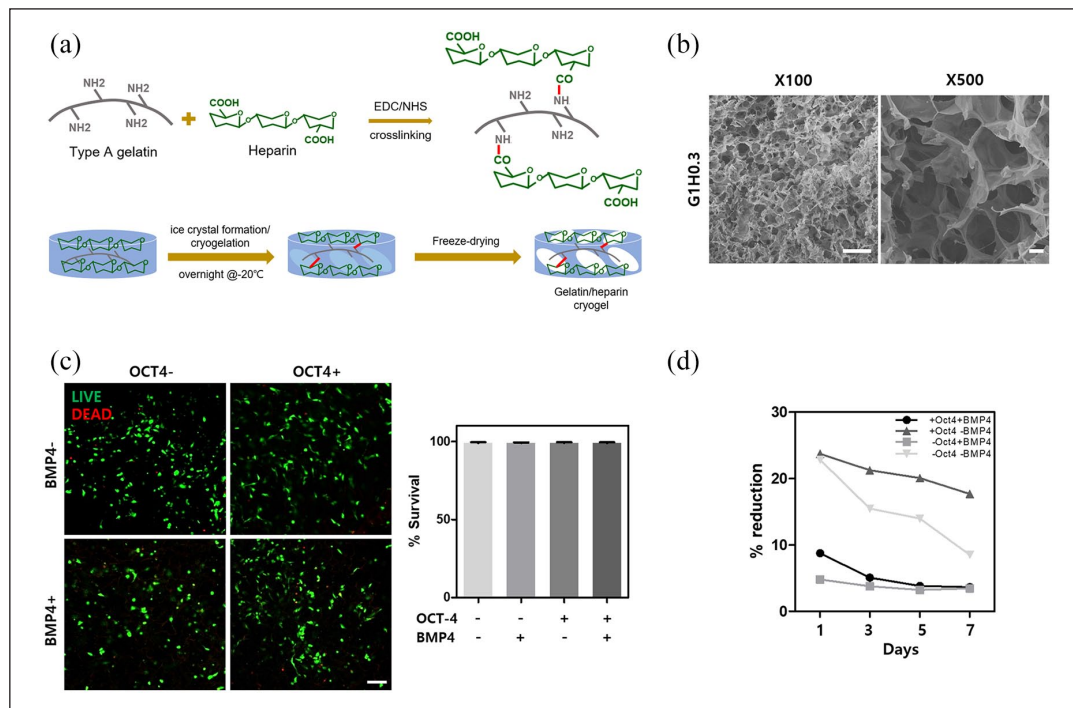


Figure 3. Characterization of gelatin-heparin cryogel and cytotoxicity and cell metabolism measurement for cell-seeded scaffolds. (a) Schematics showing fabrication method of GH cryogels. (b) Porosity measured with SEM. (c) Live and dead images 24h after cell seeding show scaffolds are not cytotoxic and quantification of live and dead staining. (d) Cell metabolism changing during 7 days of culture in osteogenic media. HUVECs treated or not treated with either OCT-4 or BMP4 are represented with - or + sign. Error bars show standard deviation on the mean for $n=3$; * $p < 0.05$; ** $p < 0.01$; *** $p < 0.001$. Scale bar = 100 μm .

temporal expression of osteogenesis can be induced with exogenous *OCT-4* gene transfection.

To examine the global gene expression changes, Quant-seq was conducted for cells after 1 week of osteogenic medium culture. Results from gene set enrichment analysis (GSEA) showed upregulation of essential gene markers for osteogenic signaling pathway in cells transfected with *OCT-4* followed by BMP4 treatment compared with control HUVECs (Supplementary Table S1). These include calcium ion-binding marker, KRAS signaling pathway-related markers, positive regulation of pathway-restricted SMAD protein phosphorylation markers, TGF- β receptor-binding markers, SMAD protein signal transduction pathway markers, and regulation of pathway-restricted SMAD protein phosphorylation markers. With prolonged osteogenic media culture for 2 weeks, elevation of gene expression for all three were further exacerbated in cells transfected with *OCT-4* followed by BMP4 treatment (Figure 2(b); top). Immunocytochemistry after 2 weeks of osteogenic culture showed prominent OCN induction in cells transfected with *OCT-4* followed by BMP4 treatment and low expression in other groups (Figure 2(b); bottom, left). In addition, ARS staining at 2 weeks confirmed osteogenesis by showing the greatest amount of calcification in cells transfected with *OCT-4* followed by BMP4 treatment (Figure 2(b); top, right). Concentrations of DNA from cells at week 2 were

measured and showed no significant difference between groups, suggesting that cells were in the same conditions at the time of staining (Figure 2(b); bottom, right). Collectively, these results suggest the ability of HUVECs to serve as an alternative cell source for osteoblasts through a transdifferentiation process.

Viability and cell metabolism of initially conditioned HUVECs on GH gels

For effective in vivo cell delivery and bone tissue formation, macroporous 1% gelatin, 0.3% (w/v) heparin (GH) cryogel, was utilized for in vivo animal study (Figure 3(a)). Before application for in vivo model, characteristics of GH scaffold were measured. GH cryogel was fabricated by crosslinking type A gelatin and heparin through EDC/NHS reaction in subzero degree condition, then freeze drying to obtain macropores. Scanning electron microscope images confirm macroporous structure of GH cryogel (Figure 3(b)). Young's modulus of average trabecular bone is 10.4 ± 3.5 GPa and that of cortical bone is 18.6 ± 3.5 GPa.²¹ However, owing to macroporous structure of GH cryogels, elastic modulus measured was 536 ± 0.05174 Pa (Supplementary Table S2). After confirming the possibility of transdifferentiation from endothelial cells into osteogenic cell types in vitro, cells were seeded on GH scaffold (Figure 3(a)). Then, cells

seeded on scaffolds were tested for viability and cell metabolism (Figure 3(c) and (d)). During 7 days of measuring cell metabolism, cells from all groups were cultured in osteogenic media. No change in percent reduction of cell metabolism in *OCT-4*-only, BMP4-only cells, and cells transfected with *OCT-4* followed by BMP4 treatment were observed, displaying no further cell proliferation. In contrast, non-treatment cells showed more than 10% decrease in cell metabolism, implying that these cells do not have plasticity to adjust in differentiation media. Live and dead staining was performed on scaffold seeded cells 24 h after seeding. Viability for all cell types did not show significant amount of cell death (Figure 3(c)). Live/dead images and quantification of those images suggest the scaffolds are not cytotoxic and thus maintain viability of all groups of cells.

Bone regeneration analysis on in vivo cranial defect mouse model

A successful bone regeneration can be achieved when both vasculogenesis and osteogenesis occur. Seeding cells on macroporous GH scaffold provides three-dimensional (3D) environment for bone formation. Due to the macroporosity, cell migration and vasculature formation along with 3D microenvironment can stimulate bone differentiation.^{19,22,23} To assess the bone tissue formation in in vivo settings, scaffolds seeded with four different groups of cells and an acellular scaffold (sham) were placed over the cranial defect area. After 8 weeks, bone formation was analyzed with micro-CT (Figure 4(a)). Quantification of micro-CT result showed that cells transfected with *OCT-4* followed by BMP4 treatment had the most amount of calcification ($16\% \pm 2.5\%$ BV/TV) (Figure 4(b)). H&E staining and Masson's trichrome staining confirmed the micro-CT data and showed higher tissue formations in sample groups transfected with *OCT-4* followed by BMP4 treatment than other groups (Figure S2 and Figure 4(c)). These staining also showed thicker tissue formation in samples transfected with *OCT-4*-only and cells transfected with *OCT-4* followed by BMP4 treatment compared with control HUVEC and BMP4 treatment-only groups (Figure 4(c)). Masson's trichrome staining, in particular, demonstrated that the newly formed bone tissue morphology was similar to that of pre-existing bone tissue. Immunohistochemistry confirmed OCN-positive human cell infiltration into new bone tissue regeneration (Figure 4(d)). In addition, CD31 staining confirmed vascularization of the newly formed bone tissue (Figure 4(d)). These in vivo results show that cells transfected with *OCT-4* followed by BMP4 treatment are incorporated and actively participated in bone regeneration in animal model. In addition, successful new bone formation from cells transfected with *OCT-4* followed by BMP4 treatment confirms enhanced bone tissue regeneration can be achieved with a single cell source.

Discussion

Engineering a bone tissue encompassing both vascular and osteogenic components is rather difficult using a single cell source. In addition, limitation in cell sources has been a large barrier in cell-based therapy until cell reprogramming technology became available. Several approaches to engineer complex bone tissues have been examined. These include seeding multiple cell types (i.e. endothelial cells, fibroblasts, and osteoblasts) to engineer vascularized bone tissues. Others have approached in way to recruit host vasculature via incorporating vascular endothelial growth factor (VEGF)-releasing scaffolds to engineered vascularized bone. In our approach, we have developed to engineer vascularized bone tissues from endothelial cells. In our study, HUVECs with both angiogenic and osteogenic characteristics were derived from *OCT-4* transfection followed by BMP4 treatment. The dual characteristics in these cells seem to be induced as a result of heterogeneous response after *OCT-4* transfection or heterogeneity induced by BMP4 treatment. Our study is in line with the previous studies showing induction of intermediate EndMT phenotype in which increased endothelial phenotype is shown as well as elevated EndMT markers after TGF- β 2 treatments in aortic valve endothelial cells, human coronary artery, and microvascular pulmonary artery endothelial cells.^{24,25} Our finding also suggests a partial EndMT state that provides the benefit of having both high endothelial and mesenchymal characteristics.

Another advantage of the intermediate state of cells transfected with *OCT-4* followed by BMP4 treatment is higher cell viability in differentiation medium compared with negative control HUVECs. Cells with *OCT-4* transfection followed by BMP4 treatment survived change in medium, inferring that EndMT state can cause cells to become adaptable to different microenvironment. Thus, osteogenic potential of directly converted cells may also increase and accompany with higher viability and adaptability of cells. Exposure to in vivo bone environment to cells with adaptable characteristics would generate better quality of engineered bone.

RNA sequencing at day 7 showed increased regulation in several molecular signaling pathways when compared with control HUVECs. Gene sets such as calcium ion binding implicate a higher selective and non-covalent interaction with calcium ions (Ca^{2+}) for cells transfected with *OCT-4* followed by BMP4 treatment. KRAS pathway-related marker upregulation suggests increased *ERK1/2* expression which is known to be eventually resulting in osteogenic differentiation.²⁶ Other SMAD protein regulation and phosphorylation and TGF- β receptor binding marker expressions represent activation of osteogenesis-related pathways. Clustering result of RNA-seq data from cells transfected with *OCT-4* followed by BMP4 treatment demonstrates both the data

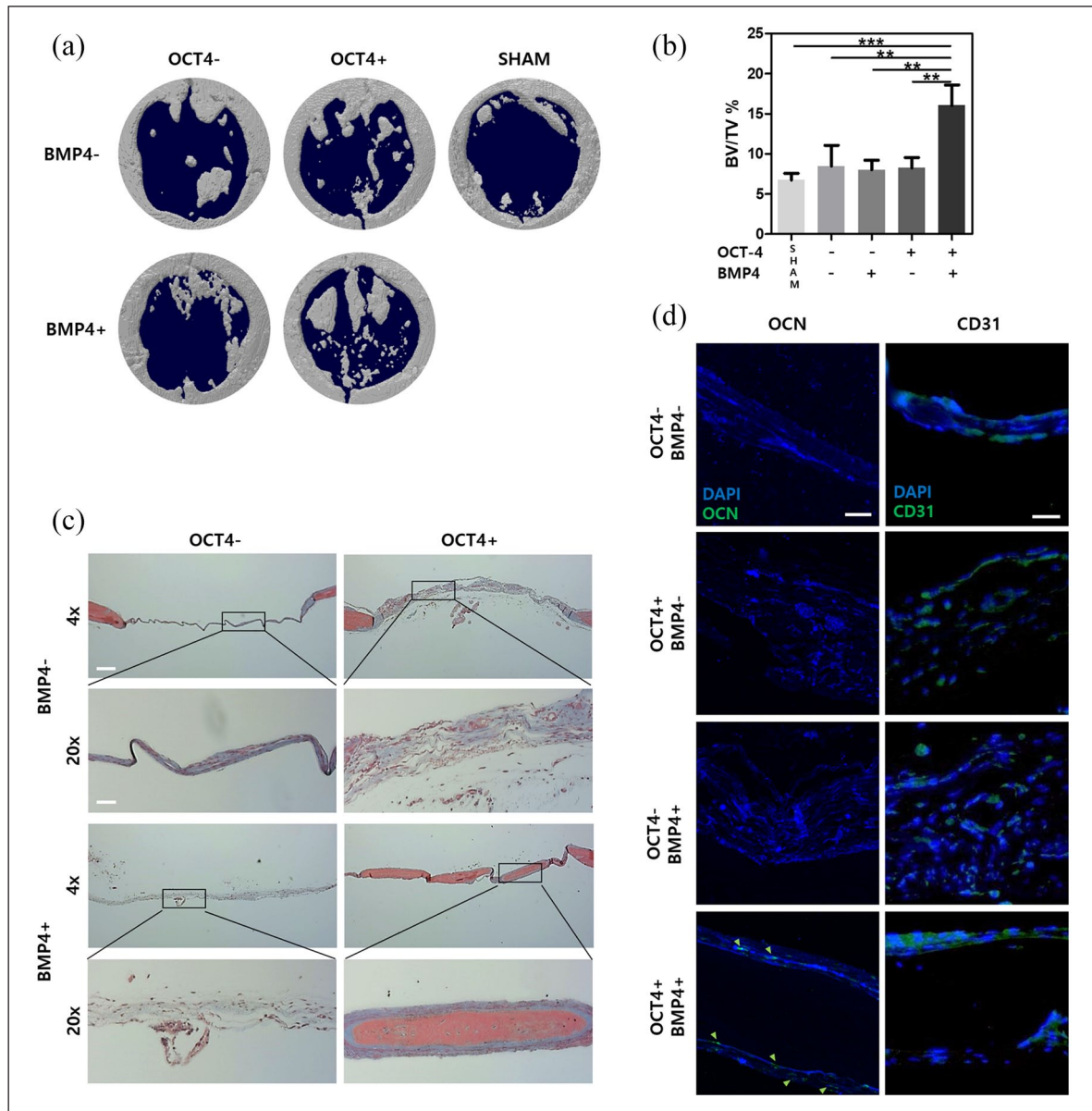


Figure 4. Sequential treatment of OCT-4 and BMP4 enhances in vivo osteogenic differentiation. (a) Micro-CT images show co-treated cells induce high bone regeneration. (b) Quantification of micro-CT bone regeneration volume. (c) MTC staining images represent defect area 8 weeks after scaffold delivery. (d) Immunohistochemistry staining images show OCN and CD31 presence in defect area 8 weeks after scaffold delivery. Green arrows indicate presence of human-specific OCN. HUVECs treated or not treated with either OCT-4 or BMP4 are represented with - or + sign. Error bars show standard deviation on the mean for $n=3$; * $p < 0.05$; ** $p < 0.01$; *** $p < 0.001$. MTC staining 4 \times , 20 \times scale bar = 200 μm , 50 μm , respectively. IHC scale bar = 20 μm .

reliability between the replicates and recapitulating the previous reports on the HUVECs undergoing EndMT via treatment of BMP4.

Lately, the importance of vascularized bone tissue engineering has been highlighted by many researchers.^{27–30} Vascularization is essential for maintaining bone homeostasis and remodeling because of its metabolic nature.³⁰ Thus, having both endothelial and mesenchymal characteristics may serve as a possible reason for enhanced osteogenesis

in our in vivo mouse model. Masson's trichrome (MTC) staining of bone tissue containing cells transfected with *OCT-4* followed by BMP4 treatment shows muscle fibers (red) wrapped in collagen (blue) which is different from non-treatment, *OCT-4*-only, and BMP4-only groups which show only thin layer of collagen and the sham group with no collagen. The structure of regenerated bone in bone tissue containing cells transfected with *OCT-4* followed by BMP4 treatment is very similar to that of the original mouse

cranial bone that can be observed in far right of the same group's 4× MTC staining. The IHC staining also suggests that this similar structure to natural bone is concentrated with human cells that were seeded onto scaffold. As stated earlier, we presume dual characteristics of endothelium and fibroblast in cells transfected with *OCT-4* followed by BMP4 treatment contributed to both angiogenesis and osteogenesis of defect area producing a richer bone structure. However, there needs to be further characterization of these cells.

Another important contributor in enhanced new bone formation in in vivo study is GH cryogel. Macroporous structure of cryogel provides favorable cell niche for seeded cells, and heparin has specific affinity with growth factors essential in osteogenesis such as VEGF and bone morphogenic protein 2 (BMP2).^{31–34} Previous study has shown GH cryogel-promoting vascularization in mouse hind limb ischemic model.¹⁹ Dual characteristics of cells transfected with *OCT-4* followed by BMP4 treatment seem to enhance from application of vascularization-promoting GH cryogels. In conclusion, our study reveals possible direct convergence from endothelial cells into osteogenic cells in vitro and in vivo. Our in vivo results suggested enhanced new bone formation which often requires multiple cell sources. Collectively, we here provide a protocol that can regenerate defected bone with single cell source, HUVECs.

Author contributions

S.H.L.K. performed all experiments, obtained and analyzed data, performed statistical analysis, and prepared the manuscript. S.S.L. and I.K. prepared cryogel scaffolds, obtained data needed regarding the scaffolds, and assisted in animal experiments. J.K. and S.K. assisted in in vivo experiments. T.B. and J.H. performed experiments needed before RNA-seq analysis. H.L. analyzed RNA-seq data and assisted in writing the manuscript. H.L. and N.S.H. conceptualized the project, supervised the work, and wrote the manuscript.

Declaration of conflicting interests

The author(s) declared no potential conflicts of interest with respect to the research, authorship, and/or publication of this article.

Funding

The author(s) disclosed receipt of the following financial support for the research, authorship, and/or publication of this article: The Institute of Engineering Research at Seoul National University provided research facilities for this paper. The research was supported by the National Research Foundation of Korea Grant funded by the Korean Government (NRF-2017M3A9C6031786).

ORCID iDs

Seunghun S Lee  <https://orcid.org/0000-0002-9654-8577>

Nathaniel S Hwang  <https://orcid.org/0000-0003-3735-7727>

Supplemental material

Supplemental material for this article is available online.

References

1. Amini AR, Laurencin CT and Nukavarapu SP. Bone tissue engineering: recent advances and challenges. *Crit Rev Biomed Eng* 2012; 40(5): 363–408.
2. Zhang R, Gao Z, Geng W, et al. Engineering vascularized bone graft with osteogenic and angiogenic lineage differentiated bone marrow mesenchymal stem cells. *Artif Organs* 2012; 36(12): 1036–1046.
3. Jiang XR, Yang HY, Zhang XX, et al. Repair of bone defects with prefabricated vascularized bone grafts and double-labeled bone marrow-derived mesenchymal stem cells in a rat model. *Sci Rep* 2017; 7: 39431.
4. Tsigkou O, Pomerantseva I, Spencer JA, et al. Engineered vascularized bone grafts. *Proc Natl Acad Sci USA* 2010; 107: 3311–3316.
5. Kang Y, Ren L and Yang Y. Engineering vascularized bone grafts by integrating a biomimetic periosteum and beta-TCP scaffold. *ACS Appl Mater Interfaces* 2014; 6(12): 9622–9633.
6. Liu Y, Chan JK and Teoh SH. Review of vascularised bone tissue-engineering strategies with a focus on co-culture systems. *J Tissue Eng Regen Med* 2015; 9(2): 85–105.
7. Takahashi K, Tanabe K, Ohnuki M, et al. Induction of pluripotent stem cells from adult human fibroblasts by defined factors. *Cell* 2007; 131(5): 861–872.
8. Patel M and Yang S. Advances in reprogramming somatic cells to induced pluripotent stem cells. *Stem Cell Rev Rep* 2010; 6(3): 367–380.
9. Takahashi K and Yamanaka S. Induction of pluripotent stem cells from mouse embryonic and adult fibroblast cultures by defined factors. *Cell* 2006; 126(4): 663–676.
10. Yu J, Vodyanik MA, Smuga-Otto K, et al. Induced pluripotent stem cell lines derived from human somatic cells. *Science* 2007; 318(5858): 1917–1920.
11. Szabo E, Rampalli S, Risueño RM, et al. Direct conversion of human fibroblasts to multilineage blood progenitors. *Nature* 2010; 468: 521–526.
12. Yamamoto K, Kishida T, Sato Y, et al. Direct conversion of human fibroblasts into functional osteoblasts by defined factors. *Proc Natl Acad Sci USA* 2015; 112(19): 6152–6157.
13. Chen Y, Cheung KM, Kung HF, et al. In vivo new bone formation by direct transfer of adenoviral-mediated bone morphogenetic protein-4 gene. *Biochem Biophys Res Commun* 2002; 298(1): 121–127.
14. Nakase T, Nomura S, Yoshikawa H, et al. Transient and localized expression of bone morphogenetic protein 4 messenger RNA during fracture healing. *J Bone Miner Res* 1994; 9(5): 651–659.
15. Wright V, Peng H, Usas A, et al. BMP4-expressing muscle-derived stem cells differentiate into osteogenic lineage and improve bone healing in immunocompetent mice. *Mol Ther* 2002; 6(2): 169–178.
16. Medici D, Shore EM, Lounev VY, et al. Conversion of vascular endothelial cells into multipotent stem-like cells. *Nat Med* 2010; 16(12): 1400–1406.

17. Tripathi A, Kathuria N and Kumar A. Elastic and macroporous agarose-gelatin cryogels with isotropic and anisotropic porosity for tissue engineering. *J Biomed Mater Res A* 2009; 90(3): 680–694.
18. Kathuria N, Tripathi A, Kar KK, et al. Synthesis and characterization of elastic and macroporous chitosan-gelatin cryogels for tissue engineering. *Acta Biomater* 2009; 5(1): 406–418.
19. Kim I, Lee SS, Bae S, et al. Heparin functionalized injectable cryogel with rapid shape-recovery property for neovascularization. *Biomacromolecules* 2018; 19(6): 2257–2269.
20. Levenberg S, Rouwkema J, Macdonald M, et al. Engineering vascularized skeletal muscle tissue. *Nat Biotechnol* 2005; 23: 879–884.
21. Rho JY, Ashman RB and Turner CH. Young's modulus of trabecular and cortical bone material: ultrasonic and micro-tensile measurements. *J Biomech* 1993; 26(2): 111–119.
22. Habibovic P, Yuan H, van der Valk CM, et al. 3D microenvironment as essential element for osteoinduction by biomaterials. *Biomaterials* 2005; 26(17): 3565–3575.
23. Gao C, Peng S, Feng P, et al. Bone biomaterials and interactions with stem cells. *Bone Res* 2017; 5: 17059.
24. Pinto MT, Covas DT, Kashima S, et al. Endothelial mesenchymal transition: comparative analysis of different induction methods. *Biol Proced Online* 2016; 18: 10.
25. Paranya G, Vineberg S, Dvorin E, et al. Aortic valve endothelial cells undergo transforming growth factor-beta-mediated and non-transforming growth factor-beta-mediated transdifferentiation in vitro. *Am J Pathol* 2001; 159(4): 1335–1343.
26. Wang Q, Chen B, Cao M, et al. Response of MAPK pathway to iron oxide nanoparticles in vitro treatment promotes osteogenic differentiation of hBMSCs. *Biomaterials* 2016; 86: 11–20.
27. Ramasamy SK, Kusumbe AP, Wang L, et al. Endothelial Notch activity promotes angiogenesis and osteogenesis in bone. *Nature* 2014; 507(7492): 376–380.
28. Kusumbe AP, Ramasamy SK and Adams RH. Coupling of angiogenesis and osteogenesis by a specific vessel subtype in bone. *Nature* 2014; 507(7492): 323–328.
29. Qu D, Li J, Li Y, et al. Angiogenesis and osteogenesis enhanced by bFGF ex vivo gene therapy for bone tissue engineering in reconstruction of calvarial defects. *J Biomed Mater Res A* 2011; 96(3): 543–551.
30. Rao RR and Stegemann JP. Cell-based approaches to the engineering of vascularized bone tissue. *Cytotherapy* 2013; 15(11): 1309–1322.
31. Ashikari-Hada S, Habuchi H, Kariya Y, et al. Heparin regulates vascular endothelial growth factor165-dependent mitogenic activity, tube formation, and its receptor phosphorylation of human endothelial cells. Comparison of the effects of heparin and modified heparins. *J Biol Chem* 2005; 280(36): 31508–31515.
32. Kim SE, Song SH, Yun YP, et al. The effect of immobilization of heparin and bone morphogenic protein-2 (BMP-2) to titanium surfaces on inflammation and osteoblast function. *Biomaterials* 2011; 32(2): 366–373.
33. Krilleke D, Ng YS and Shima DT. The heparin-binding domain confers diverse functions of VEGF-A in development and disease: a structure-function study. *Biochem Soc Trans* 2009; 37(Pt 6): 1201–1206.
34. Gandhi NS and Mancera RL. Prediction of heparin binding sites in bone morphogenetic proteins (BMPs). *Biochim Biophys Acta* 2012; 1824(12): 1374–1381.